Optimum Pulse Shaping for OFDM/BFDM Systems Operating in Time Varying Multi-path Channels

Imène Trigui[1], Mohammed Siala[1], Sofiène Affes[2], Alex Stéphenne[2,3] and Hatem Boujemâa[1]
[1]SUP'COM, Cité Technologique des Communications Route de Raoued Km 3.5, 2083 Ariana
[2]INRS-ÉMT, Université du Québec, Montréal, QC, Canada
[3]Ericsson Canada, Montreal, QC, Canada

***Abstract*— In this paper, we consider a pulse shaping OFDM/BFDM system operating over a doubly dispersive channel. We propose to search the optimal pulse maximizing the signal to interference ratio (SIR). We show that the impact of interference, composed by both inter-symbol interference (ISI) and inter-carrier interference (ICI), occurring in such a system, depends crucially on time frequency localization of transmit and receive pulses. We propose to maximize the SIR, written as a ratio of two quaternary forms, by altering between transmit and receive pulse spaces both generated by Hermite Waveforms. Numerical results show that optimized BFDM systems can outperform conventional OFDM systems with respect to SIR. In fact, biorthogonality offers more freedom to design pulses improving robustness of the multi-carrier system against channel dispersion.**

I. INTRODUCTION

High bit rate transmissions over doubly dispersive channels induce ISI due to multi-path delays. By dividing the high bit rate data stream into several low bit rate data sub-streams, each modulated over a different sub-carrier, multi-carrier transmission (MC) can significantly decrease the amount of ISI. But MC transmissions suffer from ICI due to Doppler effects and frequency synchronization errors. So far, different techniques have been proposed to suppress ISI/ICI. The ISI can be suppressed by cyclically extending a rectangular shaped symbol with a cyclic prefix (CP-OFDM) [1]. Nevertheless, the used rectangular pulse shape is not adapted to highly frequency dispersive channels due to its poor frequency localization proprieties. In pulse shaping OFDM [2] a smoother and more localized pulse is used to replace the rectangular one. While pulse shaping OFDM was proposed rather early [3,4,5], only recently the design of transmit and receive pulses for BFDM (biorthogonal frequency division multiplexing) systems has been considered in more detail [6,7]. By considering biorthogonality instead of orthogonality, more localized pulses can be designed for increased dispersion robustness and system performance improvement.

In this paper, we propose to design orthogonal and biorthogonal transmit and receive pulses which are adapted to the current channel condition in order to achieve better spectral efficiency and to reduce combined ISI/ICI. Since we target robustness to ISI/ICI, well localized pulses are designed in absence of noise. Furthermore, we only focus on distorsions caused by channel dispersion so that frequency offsets could be integrated as an additional Doppler effect. While in [8] the duality of multi-carrier systems and Weyl-Heisenberg (or Gabor) frames is elaborated and applied to the design of OFDM and BFDM systems, our approach is based on linearly combining Hermite waveforms so that maximum SIR is reached.

This paper is organized as fellows: After a presentation of an OFDM/BFDM system model in section II, the theoretical computation of orthogonal and biorthogonal pulses is discussed in section III. There, an SIR formulation and methods maximizing it are provided. In section IV, performances of the optimized MC systems are assessed and performance comparison between the different OFDM/BFDM variants is provided. Finally, a conclusion is reached in Section V.

II. SYSTEM MODEL

We consider a pulse-shaping OFDM/BFDM system deploying a time frequency rectangular lattice. Data symbols are transmitted on the lattice grid points after being modulated by carrier waveforms given by:

$$g_{lm}(t) = g(t - lT)e^{j2\pi mFt} \tag{1}$$

which are time-frequency shifted versions of the normalized energy prototype pulse $g(t)$. Note that T is the OFDM symbol duration and F is the sub-carriers frequency spacing. The baseband transmit signal is given by:

$$x(t) = \sum_{l=-\infty}^{\infty} \sum_{m=0}^{N_c-1} X_{lm} g(t - lT) e^{j2\pi mFt} \tag{2}$$

where X_{lm} is a complex data symbol transmitted at time lT and sub-carrier frequency mF. The wireless channel is modelled as a random linear time varying system H. The channel output (received signal) is thus given by:

$$y(t) = H(x(t)) = \int_\nu \int_\tau h(\tau, \nu) x(t - \tau) e^{j2\pi\nu t} d\tau d\nu \tag{3}$$

where $h(\tau, \nu)$ is the delay-Doppler spread function which is a random process in (τ, ν) [9]. The statistical description of the channel is greatly simplified by the wide-sense stationary scattering (WSSUS) assumption [9]:

$$\begin{aligned} &E\{h(\tau, \nu)\} = 0, \\ &E\{h(\tau, \nu)h^*(\tau_1, \nu_1)\} = S(\tau, \nu)\delta(\tau - \tau_1)\delta(\nu - \nu_1), \end{aligned} \tag{4}$$

where $S(\tau, \nu)$ is the channel dispersion function assumed to be supported within the rectangle $[0, T_m] \times [-B_d/2, B_d/2]$, where T_m and B_d are, respectively, the delay channel spread

This full text paper was peer reviewed at the direction of IEEE Communications Society subject matter experts for publication in the IEEE GLOBECOM 2007 proceedings.

and Doppler channel spread.
We do not include an additive noise component because we are not interested in noise effects. At the receiver, the demodulator computes, for each data symbol X_{lm}, a decision variable Y_{lm} by calculating the inner product given by:

$$y_{lm} = \int y(t) f^*_{lm}(t) dt, \quad (5)$$

where $y(t)$ is the received signal and $f_{lm}(t)$ is a time-frequency shifted version of the normalized energy receive pulse $f(t)$, defined as:

$$f_{lm}(t) = f(t - lT)e^{j2\pi mFt}. \quad (6)$$

In the special case where $f(t) = g(t)$, we deal with a pulse shaping OFDM system.
In fact, we assume a centered channel since we do not delay the receive impulse by the mean channel delay $T_m/2$. Hence:

$$y_{lm} = \sum_{l_1 m_1} X_{l_1 m_1} h_{lml_1m_1}(t), \quad (7)$$

where $h_{lml_1m_1}$ represents the global channel given by:

$$h_{lml_1m_1} = \int\int h(\tau,\nu) A^*_{fg}((l_1 - l)T + \tau, (m_1 - m)F + \nu) \; e^{-j2\pi m_1 F\tau} e^{j2\pi lT\nu} e^{-j2\pi lFT(m-m_1)} d\tau d\nu, \quad (8)$$

where A_{fg} is the cross ambiguity function between $f(t)$ and $g(t)$ defined as:

$$A_{fg}(\phi,\psi) = \int f(t) g^*(t-\phi) e^{-j2\pi\psi t} dt. \quad (9)$$

III. MC PULSES AND CORRESPONDING SIR

A. Derivation for arbitrary pulses

The decision variable corresponding to the demodulating symbols X_{lm} is expressed as:

$$Y_{lm} = X_{lm} h_{lmlm} + \sum_{(l_1,m_1)\neq(l,m)} X_{l_1m_1} h_{lml_1m_1}. \quad (10)$$

The mean ISI/ICI power is defined as:

$$\sigma_I^2 = E\{| Y_{lm} - X_{lm} h_{lmlm} |^2\}, \quad (11)$$

whereas the mean power of the desired component is defined as:

$$\sigma_S^2 = E\{| X_{lm} h_{lmlm} |^2\}. \quad (12)$$

We also assume that X_{lm} are independent identically distributed (iid) data symbols with zero mean and average transmit energy E_s. We can then show that the ISI/ICI power is given by:

$$\sigma_I^2 = E_s \sum_{(l,m)\neq(0,0)} \int\int S(\tau,\nu) |A_{fg}(lT+\tau, mF+\nu)|^2 d\tau d\nu. \quad (13)$$

Similarly, the mean power of the desired component can be expressed as:

$$\sigma_S^2 = E_s \int\int S(\tau,\nu) |A_{fg}(\tau,\nu)|^2 d\tau d\nu. \quad (14)$$

Then, we define the SIR as:

$$SIR = \frac{\sigma_S^2}{\sigma_I^2}. \quad (15)$$

According to (13), for the ISI/ICI to be low, $|A_{fg}(\tau,\nu)|^2$ must be small within all time-frequency plane regions of the form $R_{lm} = [lT - T_m/2, lT + T_m/2] \times [mF - B_d/2, mF + B_d/2], (l,m) \neq (0,0)$. Such a behavior is favored by weakly dispersive channels (small delay spread T_m and Doppler spread B_d) and small time-frequency lattice densities (large time-frequency spacing product TF). Unfortunately, channel characteristics are generally out of control. While small lattice densities mean a poor modulation spectrum efficiency, larger values of TF increase the freedom in designing pulses $g(t)$ and $f(t)$ satisfying biorthogonality property. Hence, for an MC system, low ISI/ICI is favored by the use of jointly well localized pulses and the choice of the lattice density corresponds to a trade-off between spectral efficiency and freedom in the system design.

B. Regular CP-OFDM using rectangular pulse

Let us consider an OFDM system employing a cyclic prefix [1]. Here, $T = 1/F + T_g$, where T_g denotes the length of the CP. The OFDM modulator and demodulator, deploy, respectively rectangular transmit and receive pulses given by:

$$g(t) = rect_T(t), \quad (16)$$

and

$$f(t) = rect_{T-T_g}(t). \quad (17)$$

The cross ambiguity function of a CP-OFDM system is given by:

$$A_{fg}(\tau,\nu) = \int rect_{T-T_g}(t) rect^*_T(t-\tau) e^{-j2\pi\nu t} dt. \quad (18)$$

To compute the signal plus interference power Q, we integrate the periodized version of $| A_{fg}(\tau,\nu) |^2$ over the support of the channel dispersion function $S(\tau,\nu)$. Then, we omit the signal power from Q to get the interference power.
We have:

$$Q = \int\int S(\tau,\nu) \sum_{lm} | A_{fg}(lT+\tau, mF+\nu) |^2 \, d\tau d\nu. \quad (19)$$

Here, we must distinguish both cases $T_m \prec T_g$ and $T_m \succ T_g$. In the first case we compute $| A_{fg}(\tau,\nu) |^2 = T^2 sinc^2(\nu/F)$ which does not depend on τ. Then,

$$\sum_{lm} | A_{fg}(lT+\tau, mF+\nu) |^2 = T^2 \sum_m sinc^2(\nu/F + m). \quad (20)$$

Using the fact that:
$\forall \rho \succ 0, \eta \in \Re, \sum_n sinc^2(n\rho - \eta) = 1/\rho$, we verify that (20) can be calculated using the aforementioned formula by setting ρ at 1 and η at $-\nu/F$. Hence, Q derives as:

$$Q = T^2 \int\int S(\tau,\nu) d\tau d\nu = T^2 S(0,0), \quad (21)$$

where $S(0,0)$ is the channel power.
To get the useful signal power, we compute:

$$\begin{aligned} Q_1 &= \int\int \mid A_{fg}(\tau,\nu) \mid^2 S(\tau,\nu) d\tau d\nu \\ &= T^2 \int sinc^2(\nu/F) S(\nu) d\nu, \end{aligned} \quad (22)$$

where $S(\nu) = \int S(\tau,\nu)d\tau$ is the Doppler spectrum of the channel.
Hence, the signal to interference ratio is given by :

$$SIR = \frac{Q_1}{Q - Q_1} = \frac{\int sinc^2(\nu/F) S^n(\nu) d\nu}{1 - \int sinc^2(\nu/F) S^n(\nu) d\nu}, \quad (23)$$

where $S^n(\tau,\nu) = S(\tau,\nu)/S(0,0)$, is the normalized power channel dispersion function. For the case when $Tm \succeq T_g$, a more complicated calculus is derived leading to the SIR expression given by:

$$SIR = \frac{Q}{T^2 - Q}, \quad (24)$$

where

$$\begin{aligned} Q = &4T^2 \int_0^{B_d/2} \int_0^{T_m/2} sinc^2(\nu/F) S^n(\tau,\nu) d\tau d\nu \\ &+4 \int_0^{B_d/2} \int_{T_g/2}^{T_m/2} (T - T_g/2 - \tau) \\ &sinc^2(\nu(T - T_g/2 - \tau)) S^n(\tau,\nu) d\tau d\nu. \end{aligned} \quad (25)$$

C. SIR optimized Hermite-based pulses

In this section, we present several methods for the optimization of the transmit and the receive pulses in the OFDM/BFDM system. The optimality criterion amounts to maximizing the SIR given in section 3.1. The optimum pulse is efficiently searched as combination of Hermite waveforms $u_k(t), k \succeq 0$. The rationale behind employing Hermite waveforms is that the first Hermite waveform is the Gaussian function and the k-th Hermite waveform $u_k(t)$ is the most localized function orthogonal to $u_0(t), u_1(t)...u_{k-1}(t)$. Hermite waveforms are known to be an orthonormal base of the Hilbertian space of square integrable functions, and to provide, in decreasing order, maximum localization in time and frequency. Hence all candidate pulses are expressed as a linear combination of Hermite waveforms:

$$g(t) = \sum_k \alpha_k u_k(t) \text{ and } f(t) = \sum_p \beta_p u_p(t). \quad (26)$$

As noticed in [10] from simulation results, the optimum pulse coefficients α_k, and similarly β_k, decrease exponentially with respect to k. Hence, for complexity reasons, we truncate the representation of candidate pulses to the N most concentrated Hermite waveforms. The optimization task amounts, then, to finding $\{\alpha_k\}_{k=0}^{k=N-1}$ and $\{\beta_k\}_{k=0}^{k=N-1}$ so that the target function $SIR = \sigma_s^2/\sigma_I^2$ is maximized. Using the pulse expressions below, we can formulate the cross-ambiguity function as:

$$A_{fg}(\tau,\nu) = \sum_{k=0}^{N-1} \sum_{p=0}^{N-1} \alpha_k^* \beta_p A_{kp}(\tau,\nu), \quad (27)$$

where A_{kp} is the cross-ambiguity of $u_k(t)$ and $u_p(t)$ [10]:

$$A_{kp} = \int u_p(t) u_k^*(t-\tau) e^{-j2\pi\nu t} dt. \quad (28)$$

A_{kp} can be expressed as:

$$\begin{aligned} A_{kp}(\tau,\nu) = &(-1)^{k+p} \sqrt{\tfrac{p!}{k!}} e^{-\frac{1}{2}(\tau^2+\nu^2)} (\sqrt{\pi})^{k-p} \\ &(\tau + i\nu)^{k-p} L_p^{(k-p)}(\pi(\tau^2+\nu^2)), \end{aligned} \quad (29)$$

where

$$L_b^a(x) = \sum_{i=0}^{b} \frac{b!(-1)^i x^i}{i!(b-i)!} \prod_{k=i+1}^{b} (k+a) \quad (30)$$

is the generalized Laguerre polynomial.
Based on that, the signal power becomes:

$$\sigma_S^2 = E_s \sum_{k,p \le N-1} \sum_{k_1,p_1 \le N-1} \alpha_k^* \beta_p \alpha_{k_1} \beta_{p_1}^* D(k,p,k_1,p_1), \quad (31)$$

where:

$$D(k,p,k_1,p_1) = \int\int S(\tau,\nu) A_{kp}(\tau,\nu) A_{k_1p_1}^*(\tau,\nu) d\tau d\nu. \quad (32)$$

Similarly, the mean interference power is written as:

$$\sigma_I^2 = E_s \sum_{k,p \le N-1} \sum_{k_1,p_1 \le N-1} \alpha_k^* \beta_p \alpha_{k_1} \beta_{p_1}^* I(k,p,k_1,p_1), \quad (33)$$

where :

$$\begin{aligned} I(k,p,k_1,p_1) = &\int\int S(\tau,\nu) \textstyle\sum_{(l,m)\neq(0,0)} \\ &A_{kp}(lT+\tau, mF+\nu) A_{k_1p_1}^*(lT+\tau, mF+\nu) d\tau d\nu. \end{aligned} \quad (34)$$

Let $U^T = [\alpha_0 ... \alpha_{N-1}]$ and $V^T = [\beta_0 ... \beta_{N-1}]$, then the SIR becomes:

$$SIR = \frac{(U \otimes V^*)^H D (U \otimes V^*)}{(U \otimes V^*)^H I (U \otimes V^*)}, \quad (35)$$

where $\otimes$ is the Kronecker tensor product, D is a $(N^2 \times N^2)$ hermitian matrix of elements $D(k,p,k_1,p_1)$ and I is a $(N^2 \times N^2)$ hermitian positive matrix of elements $I(k,p,k_1,p_1)$. Formulated as below, the SIR is the target function to be maximized so that optimal pulses are reached. Next we present pulse design algorithms for both orthogonal and biorthogonal cases based on SIR maximization. In the orthogoanal case, optimal pulse search is done in one Hermite generated space since transmit and received pulses are the same. In the biorthogonal case, optimal pulse search is done by exploring two different Hermite generated spaces to get the optimal coefficients U and V and therefore, $g(t)$ and $f(t)$.

1) Optimization of biorthogonal receive and transmit pulses (PS-BFDM): The optimization procedure is based on altering between transmit and receive Hermite generated spaces by iteratively and alternatively fixing the transmit and the receive pulse to optimize the other. By fixing either U or V, the SIR becomes a ratio of two quadratic forms easy to optimize. In the initialization step, we begin by setting V or U at a random vector. In the i-the iteration, the optimal achievable SIR corresponds to the maximum generalized eigenvalue of the pair of symmetric matrices $(D_1^{(i)}, I_1^{(i)})$ given by:

$$\begin{aligned} \lambda_{max}(D_1^{(i)}, I_1^{(i)}) &= \sup \tfrac{U^H D_1^{(i)} U}{U^H I_1^{(i)} U} \\ &= \sup\{\lambda / det(\lambda I_1^{(i)} - D_1^{(i)}) = 0\}, \end{aligned} \quad (36)$$

where $D_1^{(i)}$ (respectively $I_1^{(i)}$) is the entry-wise product of D (respectively I) by $V^{(i)^*}V^{(i)^T}$. Since transmit and receive pulses have symmetric roles, we always set $V^{(i+1)}$ at the obtained vector U in the i-th iteration. The convergence of this procedure is interpreted as a precision on the maximum achievable SIR relative to the initialization value. Thus, the global maximum can be reached by using many different random initializations. Moreover, by simulation tests, we show that by increasing the iteration number, local maxima can be avoided and the algorithm converges to the global maximum of the target function.

2) Optimization of orthogonal pulses (PS-OFDM): Here we deal with an orthogonal system deploying the same pulse shape in transmission and reception, i.e. $g(t) = f(t)$. The SIR becomes a ratio of two quaternary forms with respect to $U = V$. While optimizing the SIR with respect to U is rather hard, we opt for a constrained maximization with respect to the $(N^2 \times 1)$ vector $\xi = U \otimes U^*$ which element number $kN+p$ is $\{\alpha_k \alpha_p^*\}$. The cost function is $\psi(\xi) = \frac{\sigma_s^2}{\sigma_I^2} = \frac{\xi^H D \xi}{\xi^H I \xi}$. Hence, σ_s^2 and σ_I^2 are quadratic forms in ξ. The projected gradient algorithm is used for a constrained optimization of the pulse shape $g(t)$ with respect to ξ. The optimum solution is reached by iteratively computing:

$$\alpha_k^{(i+1)} = \alpha_k^{(i)} + \eta C(k), \tag{37}$$

where:

$$C^T = (J_\xi^T J_\xi)^{-1} J_\xi^T \overrightarrow{\nabla}_\xi \psi, \tag{38}$$

η is a positive multiplicative factor and J_ξ is the Jacobian matrix of ξ with respect to $\{\alpha_k\}_{k=0}^{N-1}$ at $\{\alpha_k^{(i)}\}_{k=0}^{N-1}$. Note that in this section we suppose real-valued pulses so that we can compute the Jacobian matrix. Otherwise more complicated derivations are necessary.

IV. Numerical Results

We consider a pulse shaping OFDM/BFDM system using a time frequency lattice with $TF \succ 1$, transmitting over a WSSUS channel. For simplicity, we consider a constant square-shaped channel scattering function with $T_m = B_d = \sqrt{\beta}$, where β is the channel spread factor. Moreover, for evident symmetry reasons with respect to Doppler and delay spread characteristics, we assume the time-frequency lattice to be square-shaped, with equal carrier separation and symbol period $T = F = \sqrt{TF}$, where $TF = 1/\delta$ and δ is the lattice density. Due to the $\pi/2$ rotational invariance of the rectangular lattice, the most localized prototype function should be searched among all orthonormal prototype functions with $\pi/2$ rotational invariant ambiguity functions [11]. To achieve this, we require the ambiguity function of each candidate function to be also invariant to a $\pi/2$ rotation. As shown in (27), To guarantee the $\pi/2$ rotational invariance of $A_{fg}(\tau, \nu)$, we should keep in (26) only Hermite waveforms for which the cross-ambiguities $A_{kp}(\tau, \nu)$ are also $\pi/2$ rotational invariant. By examining the expression of $A_{kp}(\tau, \nu)$ in (29), we see that rotational invariance is guaranteed whenever $p - k$ modulo 4 is 0. Then, both p and k can be written as $4c + l, l = 0, 1, 2, 3,$ and c is any

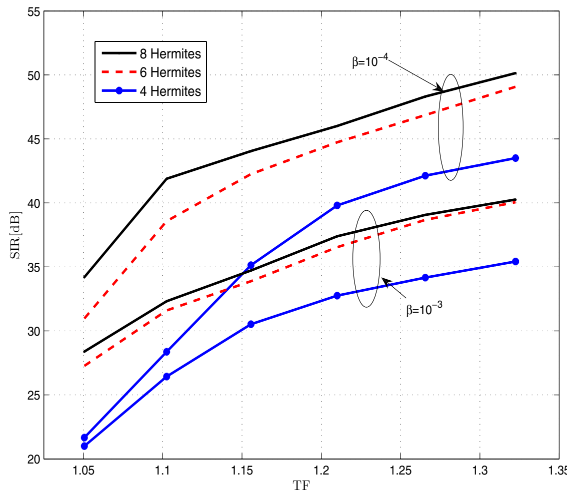

Fig. 1. PS-BFDM optimized SIR as a function of TF with increased number of Hermite waveforms .

non-negative integer. Since we want to keep the most localized Gaussian function in the representation of all candidate pulses, we should choose $l = 0$. Hence, we express $g(t)$, and similarly $f(t)$ as:

$$g(t) = \sum_k \alpha_{4k} u_{4k}(t) \text{ and } f(t) = \sum_p \beta_{4p} u_{4p}(t). \tag{39}$$

Simulation number one aims at finding the optimal computational size N of the subset of Hermite waveforms with indices multiple of four used to form optimal biorthogonal pulses. In figure 1, we show that BFDM system performance in terms of SIR is greatly improved while increasing the number N of Hermite waveforms. Nevertheless, this SIR improvement decreases with N. Adding to that the fact that increasing N induces computational complexity and even causes instability in the optimization algorithm , we choose $N = 8$ as an optimal size offering good SIR level and acceptable algorithm complexity. In figure 2, we present an exemple of optimized biorthogonal pulses in transmission and reception for a lattice density $\delta = 0.8$ and a channel dispersion $\beta = 10^{-3}$. In figure 3, we compare optimized PS-OFDM and PS-BFDM system performances using eight Hermite waveforms. The use of biorthogonal pulses improves visibly the SIR for high lattice densities (low values of TF approaching 1). In fact, biorthogonality offer more freedom to design more localized pulses with greater capability to overcome channel dispersion. The difference in performance between BFDM and OFDM vanishes for small lattice densities (large values of TF, far from 1). In figure 4, we compare our optimized PS-BFDM design with a conventional state-of-the-art CP-OFDM system which both are biorthogonal modulations deploying, respectively, well and poor frequency localized pulses. We show the SIR obtained with the two systems as a function of the normalized maximum Doppler frequency for three different normalized channel delay spread values. The CP-OFDM system deploys a cyclic prefix (CP) of

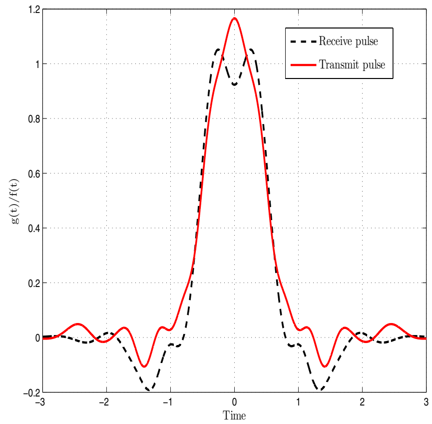

Fig. 2. Transmit and receive pulses for $\delta = 0.8$ and $\beta = 10^{-3}$.

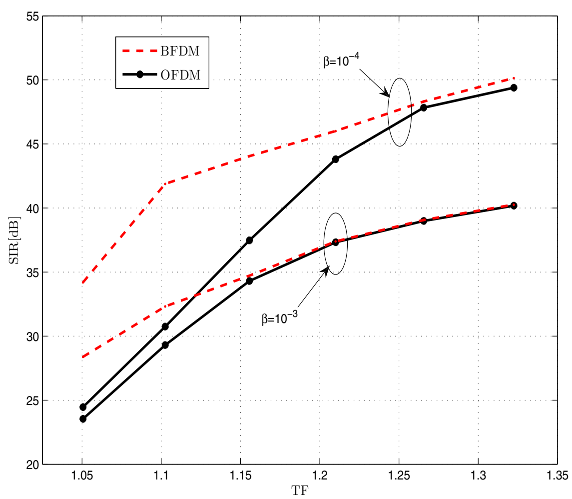

Fig. 3. PS-BFDM/PS-OFDM performances comparison .

length $T_g = 0.25T$ which corresponds to $TF = 1.25$ for both systems. A BFDM system outperforms a CP-OFDM system for a large range of channel dispersion, especially in the case of a highly frequency dispersive channel thanks to the use of well frequency localized pulses. When $T_m = T_g$, the CP-OFDM system might slightly outperform the BFDM system when the Doppler spread vanishes (slowly varying channel). However, since we have a trend for higher mobility, then the aforementioned situation is not frequent. Moreover, since a rectangular pulse is the combination of an infinite number of hermite waveforms, the performance limitation of BFDM systems when $T_m = T_g$ can be overcome by increasing N. Algorithm complexity can be accepted since we design the optimal pulse only once, offline.

V. Conclusion

For wireless communications over fast varying channels, pulse-shaping multi-carrier systems achieve lower interference than the CP-OFDM system, because pulse shaping avoids the poor spectral concentration of the rectangular pulse employed

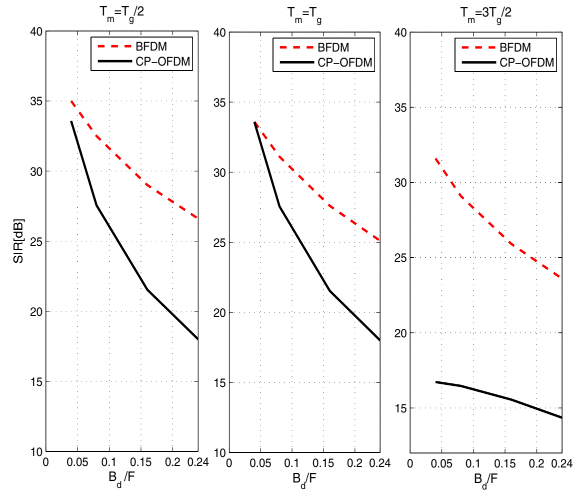

Fig. 4. PS-BFDM/CP-OFDM performances comparison .

by CP-OFDM. To leverage this advantage, it is necessary to design well time-frequency localized transmit and receive pulses in accordance with the statistical properties of the wireless channel. In this paper, we proposed pulse optimization techniques maximizing the SIR for given channel statistics. We have shown that a PS-BFDM system outperforms both PS-OFDM and CP-OFDM systems for high spectral efficiency and for a large range of channel dispersion.

References

[1] A. Peled and A. Ruiz, " Frequency domain data transmission using reduced computational complexity algorithms," *in Proc. IEEE ICASSP-80, (Denver, CO),* pp. 964-967, 1980.

[2] R. Haas and J.C. Belfiore, "A time frequency well localized pulse for multiple carrier transmission," *Wireless Personal Communications,* vol. 5, pp. 1-18, 1997.

[3] B. R. Saltzberg, "Performance of an efficient parallel data transmission system," *IEEE Trans. Comm. Technol.,* vol. 15, pp. 805-811, Dec. 1967.

[4] H. Bölcskei, P. Duhamel, and R. Hleiss, "Design of pulse shaping OFDM/OQAM systems for high data-rate transmission over wireless channels," *in Proc. of IEEE International Conference on Communications (ICC), Vancouver, BC, Canada,* vol. 1, pp. 559-564, June 1999.

[5] T. Strohmer and S. Beaver, "Optimal OFDM Design for Time-Frequency Dispesive Channels," *IEEE Transactions on Communications,* vol. 51, pp. 1111-1123, Jul. 2003.

[6] D. Schafhuber, G. Matz, and F. Hlawatsch, "Pulse-shaping OFDM/BFDM systems for time-varying channels: ISI/ICI analysis, optimal pulse design, and efficient implementation, " *in Proc. IEEE PIMRC-02, (Lisbon, Portugal),* pp. 1012-1016, Sept. 2002.

[7] W. Kozek and A.F. Molisch, "Nonorthogonal pulseshapes for multicarrier communications in doubly dispersive channels," *IEEE JSAC,* vol. 16, pp. 1579-1589, Oct. 1998.

[8] H. Bölcskei, "Efficient design of pulse shaping filters for OFDM systems," *in Proc. SPIE Wavelet Applications in Signal and Image Processing VII, (Denver, CO),* pp. 625-636, July 1999.

[9] P. A. Bello, "Characterization of randomly time-variant linear channels," *IEEE Trans. Comm. Syst.,* vol. 11, pp. 360-393, 1963.

[10] T. Kurt, M. Siala and A. Yongaoglu, "Multi-carrier signal shaping employing Hermite functions,“ *13th European Signal Processing Conference (EUSIPCO05), Antalya, Turkey,* September 4-8, 2005.

[11] R. Haas, "Application des transmissions porteuses multiples aux communications radio mobiles," *Thesis Report (In English), ENST Paris, France,* January 26, 1996.